Hindawi
International Journal of Electrochemistry
Volume 2018, Article ID 1697956, 6 pages
https://doi.org/10.1155/2018/1697956

Research Article

Impact of Various Acids and Bases on the Voltammetric Response of Platinum Group Metal Oxides

Sebastian Chalupczok, Peter Kurzweil, and Helmut Hartmann

Electrochemistry Laboratory, University of Applied Sciences, Kaiser-Wilhelm-Ring 23, 92224 Amberg, Germany

Correspondence should be addressed to Peter Kurzweil; p.kurzweil@oth-aw.de

Received 30 August 2017; Accepted 9 November 2017; Published 23 January 2018

Academic Editor: Davood Nematollahi

The voltammetric response of platinum metal oxides is discussed with respect to novel pH sensors combining both miniaturization and stability. For practical applications in solutions of any kind, for example, in tap water and in domestic sewage, various interferences must be considered, such as chloride and reducing agents. This work clarifies the voltammetric behavior of RuO_2 electrodes in solutions of different pH values and ionic strengths.

1. Introduction

Platinum metal oxides such as ruthenium dioxide (RuO_2) and iridium dioxide (IrO_2) are known for their electrical resistivity at room temperature and stability in aggressive solutions containing hydrofluoric acid [1]. Their redox chemistry makes them attractive for applications such as pH sensors [2–8] and supercapacitors [4, 9].

Platinum metal oxides, in contact with aqueous solutions, are able to adsorption water, whereby a carpet of hydroxyl (OH) groups is formed by proton displacement during anodic charging. Two sorts of hydrogen groups exist: OH with bridging oxygen atoms which acts as Lewis acid or base, and OH that works as a Brønsted base [10]. Protons from the solution can be exchanged with the electrode surface by following simplified equation:

$$\mathrm{Ru^{IV}O_2} + \mathrm{e^-} + \mathrm{H^+} \rightleftharpoons \mathrm{Ru^{III}O\,(OH)} \tag{1}$$

Using Nernst's equation, the redox potential of the RuO_2 electrode depends on the pH value. By definition in the solid state, the activities of Ru(III) and Ru(IV) approach $a = 1$, so that (3) is received.

$$\begin{aligned} E &= E^0 - \frac{RT}{F} \ln \frac{a\left(\mathrm{Ru^{III}}\right)}{a\left(\mathrm{Ru^{IV}}\right) \cdot a\left(\mathrm{H^+}\right)} \\ &= E^0 - \frac{\ln 10 \cdot RT}{F} \left(\mathrm{pH} + \log \frac{a\left(\mathrm{Ru^{III}}\right)}{a\left(\mathrm{Ru^{IV}}\right)} \right). \end{aligned} \tag{2}$$

At 25°C,

$$E = E^0 - 0.059 \cdot \mathrm{pH}. \tag{3}$$

The thermodynamically calculated standard potential equals $E^0 = 0.94\,\mathrm{V}$ [11]. According to the above equations, RuO_2 electrodes can be utilized for a potentiometric sensor.

Usually, buffer solutions are used to investigate the pH sensitivity, whereas the impact of ionic strength has scarcely been considered in the literature so far. At present, the redox behavior of RuO_2 in aqueous solutions is not fully understood. We present new findings on the impact of various acids and bases on the performance of RuO_2 electrodes by the help of cyclic voltammetry (CV), open circuit potential (OCP) measurements, and electrochemical impedance spectroscopy. As well, the hydrogen insertion reaction into the lattice structure of RuO_2 electrodes is considered.

2. Instruments and Methods

Electrodes were prepared by thermal spray pyrolysis from commercially available ruthenium(III) chloride hydrate (Sigma-Aldrich). The substrate, titanium foil (Ti) of 0.05 mm thickness (Ankuro Int. GmbH), was pretreated with abrasive paper and degreased with acetone to ensure good adhesion of the oxide layer. The $RuCl_3 \cdot x\,H_2O$ was solved in acetone and then decomposed on the substrate in a furnace in air at 500°C for 2 h. Our previous investigations by thermogravimetric

Table 1: Drift of the OCP (E versus RHE) of a RuO_2 electrode in various acids and bases at 25°C in the course of several days. For comparison: negative decadic logarithm of the dissociation constants of acids (pK_a) and bases (pK_b) from [12]. Theoretical potential of the reversible hydrogen electrode: V RHE = 0.059 pH (25°C).

Solution	pH (calculated)	pK (25°C)	Day 1 (E/mV)	Day 2 (E/mV)	Day 3 (E/mV)
1 M H_2SO_4	0.11	−3	920	923	920
1 M HCl	0.13	−7	815	697	850
1 M H_3PO_4	1.08	+2.13	866	889	864
1 M HNO_3	0.13	−1.37	844	806	942
1 M NaOH	13.8	−1.1	702	710	912
1 M KOH	13.8	−0.56	846	972	902

analysis revealed that the transition temperature of oxide formation is at about 360°C. The active area of the sensor was 1 cm^2, and the thickness of the oxide layer was about 2 μm.

The electrochemical measurements were carried out using a three-electrode arrangement, a potentiostat/galvanostat (EC301 Stanford Research System, Inc.), and a frequency response analyzer (Solartron SI 1250). The reference electrode (RE) was a reversible hydrogen electrode (RHE), the counterelectrode (CE) was a platinum-foil, and the working electrode (WE) was the above-mentioned RuO_2 electrode. As electrolytes, 70 mL of 1-molar solutions of sulfuric acid (H_2SO_4), hydrochloric acid (HCl), phosphoric acid (H_3PO_4), nitric acid (HNO_3), sodium hydroxide (NaOH), and potassium hydroxide (KOH) were used. The temperature was 25 ± 0.5°C.

3. Results and Discussion

3.1. Open Circuit Potential in Different Solutions. The known problems of RuO_2 electrodes in aqueous solutions are (i) potential drift and (ii) hysteresis. With respect to the pH sensitivity, the OCP of a RuO_2 electrode were observed in 1-molar acids and bases for a period of several days (see Table 1).

The titanium support plays no role, as far as RuO_2 is coated sufficiently thick. The quality of the electrode was proved by the help of microscopy and impedance spectroscopy. Any weakly conducting layer of TiO_2 on the substrate material, which might be formed by corrosion under an insufficient RuO_2 coating, causes a dramatic increase of the resistance of the electrode within several days. With respect to quality assurance, any undesired peeling off of the RuO_2 coating can easily be checked under a magnifying glass.

In H_2SO_4, the RuO_2 electrode provided a stable potential of about 920 mV RHE, which is in good agreement with the thermodynamically calculated standard potential (940 mV [11], (1)). The theoretical pH values in Table 1 were calculated using activity coefficients γ from the literature [12], pH = $-\log(\gamma c)$, for c = 1 mol/L.

Unfortunately, the potentials in HCl, HNO_3, and alkali hydroxides vary dramatically depending on the ionic composition of the solution. According to the pK_a values, HCl behaves as an extremely strong acid, followed by H_2SO_4 and HNO_3, whereas H_3PO_4 appears moderately strong. In contrast to the expectation that the strongest acid should have the highest potential, Table 1 reveals no clear trend, because the solution is determined not only by the protons, but also by the total ionic strength of all ions present. For example, RuO_2 shows a significant sensitivity to chloride. Therefore, any empirical correlation between acidity (pK_a value) and the OCP remains vague, as shown in Figure 1.

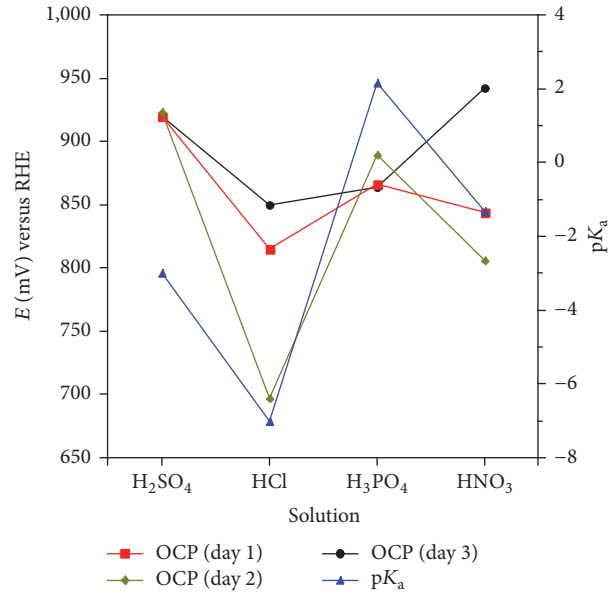

Figure 1: Fuzzy correlation of acid strength pK_a and open circuit potential of a RuO_2 electrode in different acids and bases.

Chloride ions play a special role, as they interact with the RuO_2 lattice, so that they change the open circuit potential as well as the slope dE/dpH and the cyclic voltammogram (Figure 3). Since chloride and chlorine compounds are found in municipal wastewater, the conventional potentiometric pH measurements using metal oxides are difficult.

3.2. Cyclic Voltammetry in Acidic Solutions. With respect to clarifying the electrochemical behavior of RuO_2 in different acids, cyclic voltammetry was applied. The investigation was to show changes in the voltammograms depending on the pH value. Figure 2 presents the fundamental difference between the cyclic voltammogram of a RuO_2 electrode in H_2SO_4 in contrast to NaOH.

In H_2SO_4 (pH 0.1), 14 different peaks can be distinguished besides the hydrogen and oxygen evolution reaction in the potential range between 0 and 1.4 V RHE.

At $E \approx 0$ V RHE the hydrogen adsorption reaction occurs on the onefold coordinatively unsaturated ruthenium site (in short: 1f-cus Ru) and the bridging oxygen atom. Above 0.4 V RHE the oxidation of the surface takes place. In acidic solutions the redox transitions of Ru(III) → Ru(IV) → Ru(V) → $\cdots$ → Ru(VIII) appear to be the predominant oxidation states:

$$2RuO_2 + 2H^+ + 2e^- \rightleftharpoons Ru_2O_3 + H_2O \quad (4)$$

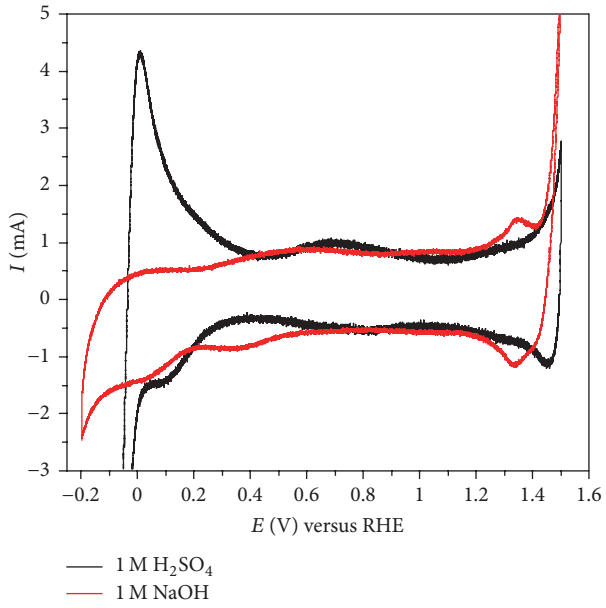

FIGURE 2: Cyclic voltammogram of a Ti/RuO_2 electrode in 1 M H_2SO_4 and 1 M NaOH at 25°C. Counterelectrode: Pt sheet. Scan rate: 100 mV/s.

$$\frac{1}{2}Ru_2O_5\,(s) + 3H^+ + e^- \rightleftharpoons Ru(OH)_2{}^{2+} + \frac{1}{2}H_2O \quad (5)$$

$$H_2RuO_5 + 3H^+ + 3e^- \rightleftharpoons \frac{1}{2}Ru_2O_5\,(s) + \frac{5}{2}H_2O \quad (6)$$

$$RuO_4{}^- + e^- \rightleftharpoons RuO_4 \quad (7)$$

Interestingly, different acids produce clearly different voltammograms (Figure 3).

Oxygen Reduction. The shapes of the anodic cycles are quite similar in different acids. However, the cathodic ramp is substantially altered by the presence of chloride in HCl. In HCl, the oxygen evolution reaction occurs at a lower potential than in the other acids. The oxygen evolution at first appears in HCl and then shifts to HNO_3, H_2SO_4, and finally H_3PO_4, whereby the electrolyte resistance plays a minor role. These low overpotentials are known for the chlorine evolution reaction in the chloralkali electrolysis with dimensionally stable anodes (TiO_2/RuO_2, DSA). According to the Deacon process, traces of chlorine might be formed by reaction with anodically generated oxygen.

$$4HCl + O_2 \rightarrow 2Cl_2 + 2H_2O \quad (8)$$

The oxygen reduction peak at about 1.1 V RHE was attributed to Ru(VIII), especially to the species RuO_4 in the measured solution, based on in situ reflectance spectroscopy in 0.5 M H_2SO_4 by Kötz et al. [13]. However, RuO_4 is formed at high positive potentials during oxygen evolution and appears to be the main corrosion product in acidic solutions (see (7)). The formation of RuO_4 in HCl is attributed to the shifted potential and therefore earlier oxygen evolution reaction.

Hydrogen Adsorption. By extending the potential window to more negative values, the hydrogen adsorption region appears more clearly and the peak heights of the anodic hydrogen oxidation increase. Starting the voltammogram at −0.1 V RHE, the largest current flows in H_2SO_4. Surprisingly, H_3PO_4 follows, comparable to HCl, whereas HNO_3 reveals the weakest current (due to the smallest hydrogen evolution current).

We conclude that hydrogen oxidation current depends on the extent of the hydrogen evolution, which can be controlled by the potential window. Assuming that the potential window of 1.53 V leads to distinct peaks in 1 M H_2SO_4, the required potential difference was not reached in 1 M HNO_3 (about 1.48 V). About 1.4 V in 1 M HCl is enough to show a pronounced voltammogram of ruthenium oxide.

The oxygen reduction reaction seems to be unaffected by the cathodically altered potential window.

3.3. Cyclic Voltammetry in Alkaline Solutions. In alkaline solution, the predominant oxidation states read Ru(III) → Ru(IV) → Ru(VI) → Ru(VII). At high potentials in the region of oxygen evolution, Ru(VIII) is generated and can be reduced in the solution at lower potentials. The redox reactions can be expressed as

$$RuO_4{}^{2-} + 4H^+ + 2e^- \rightleftharpoons RuO_2 + 2H_2O \quad (9)$$

$$RuO_4{}^- + e^- \rightleftharpoons RuO_4{}^{2-} \quad (10)$$

The cyclic voltammograms of RuO_2 in NaOH and KOH are shown in Figure 4.

Using a potential window of 0 to 1.5 V, the hydrogen oxidation region at $E \approx 0$ V is not pronounced. The shape of the voltammograms remains the same. However, there are differences in the peak heights, that is, for the Ru(VI)/Ru(VII) couple at 1.3 V. If the potential window is extended to more negative potentials, the hydrogen oxidation region becomes more intense, and peak height of the Ru(III) → Ru(IV) oxidation at 0.6 V changes too. Note that in acids, this peak was not changed (or only in a negligible extent).

3.4. Impedance Spectroscopy in Acidic and Alkaline Solutions. The RuO_2 electrode was characterized in different acidic and alkaline solutions by impedance spectroscopy in a frequency range from 65 kHz to 10 Hz. The electrochemical activity of the oxide–electrolyte interface is evaluated by the help of capacitance [14].

$$C(\omega) = \frac{\mathrm{Im}\,\underline{Y}(\omega)}{\omega} = \frac{-\,\mathrm{Im}\,\underline{Z}}{2\pi f\left|(\mathrm{Re}\,\underline{Z})^2 + (\mathrm{Im}\,\underline{Z})^2\right|}. \quad (11)$$

Figure 5 shows that the RuO_2 electrode exhibits the largest interface activity in H_2SO_4 (1450 μF/cm^2 at 10 Hz), whereas the capacitance in H_3PO_4 is the smallest (650 μF/cm^2 at 10 Hz). HCl, HNO_3, and NaOH range is around 1250 μF/cm^2.

Interface capacitance allows distinguishing strong and weak acids. Although the pK_a of HCl is the highest, the capacitance is less pronounced than that of H_2SO_4. As seen with the cyclic voltammograms, the chloride ions compete with

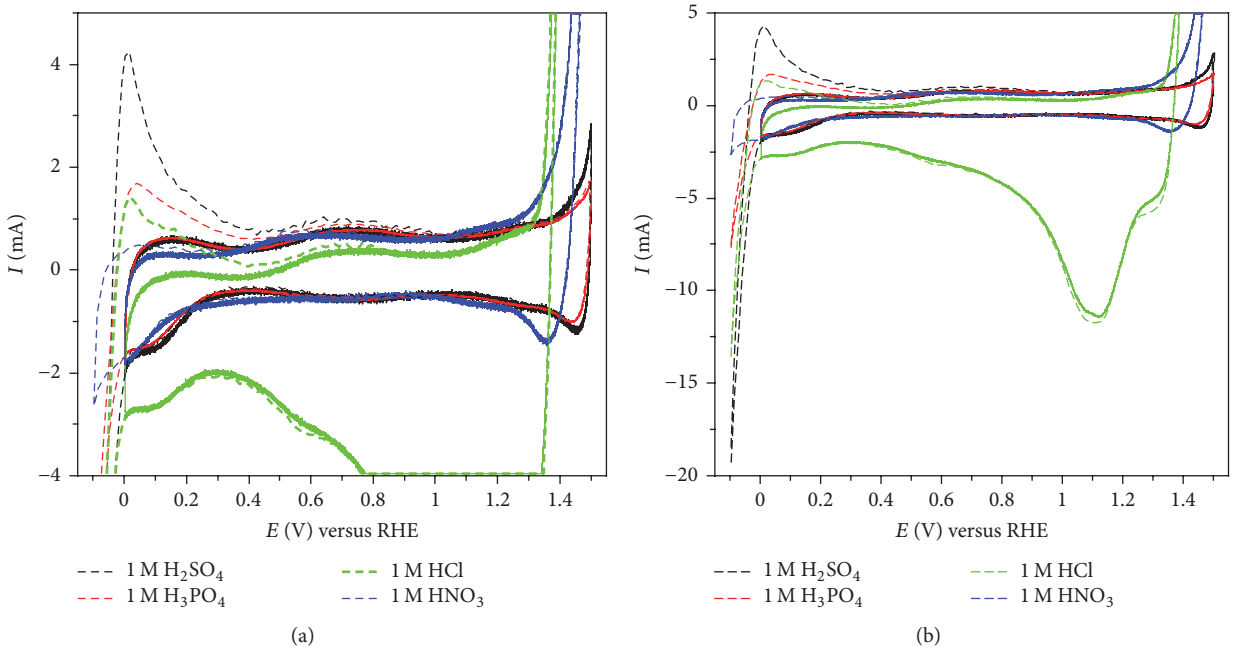

Figure 3: (a) Cyclic voltammograms of acids at 25°C. Impact of an extended potential window: solid lines: 0 to 1.5 V; dashed lines: −0.1 to 1.5 V RHE. Scan rate: 100 mV/s. (b) Full scale to show the oxygen reduction (RuO_4) and the impact of chloride at 1.1 V RHE.

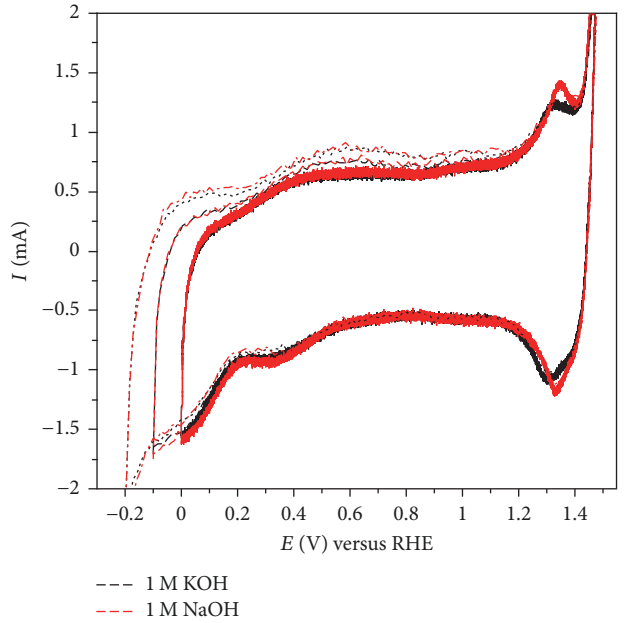

Figure 4: Cyclic voltammograms of alkali hydroxide solutions (red: 1-molar KOH; black: 1-molar NaOH). Impact of an extended potential window (solid lines: 0 to 1.5 V; dashed lines: −0.1 and −0.2 to 1.5 V). Scan rate: 100 mV/s.

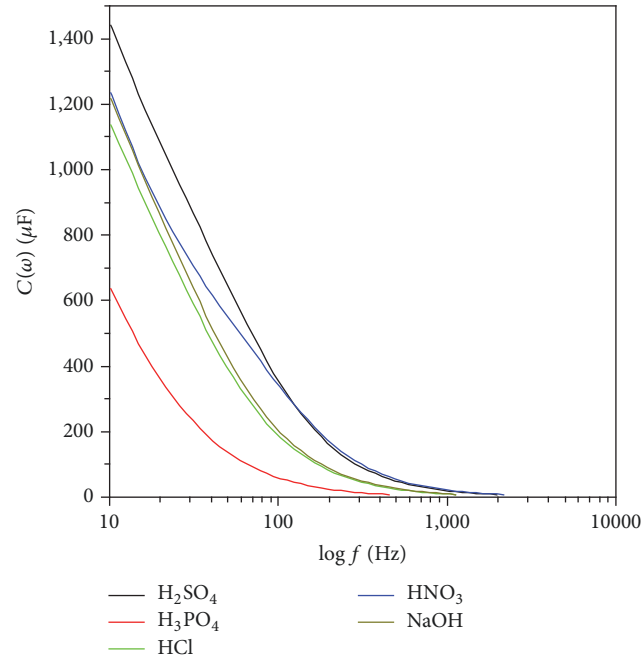

Figure 5: Frequency response of capacitance of a Ti/RuO_2 electrode (versus RHE) in different solutions at 25°C.

hydroxide sites in the RuO_2 lattice. Other ions present in the acids do not affect the behavior of the electrode, that is, sulfate, phosphate, and nitrate.

The Nernst slope, which generally deviates from 59 mV pH^{-1} (25°C), is nearly independent of dissolved anions in the solution (such as SO_4^{2-}, PO_4^{2-}, and NO_3^-). However, commercial RuO_2 resistive pastes, which contain PbO, exhibit a slope which depends on different anions significantly [15].

3.5. Proton Insertion in Ruthenium Dioxide. As shown in Figure 3, the extension of the cathodic potential window leads to a significant increase in hydrogen oxidation current at $E \approx 0$ V. This is consistent with the fact that RuO_2 forms a

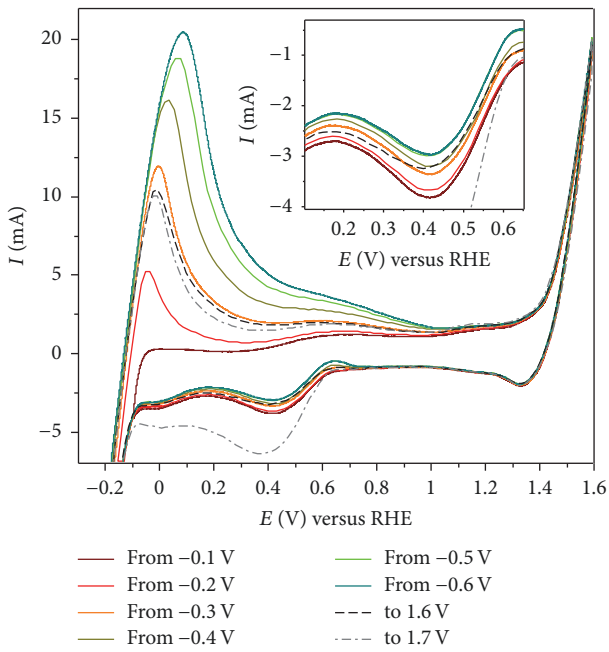

FIGURE 6: Increasing oxidation of adsorbed hydrogen (by hydrogen insertion into bulk RuO_2) in a more and more cathodic potential window (hydrogen evolution) and more positive potentials (oxygen evolution). Picture inside: Ru(IV) → Ru(III) reduction at 0.4 V.

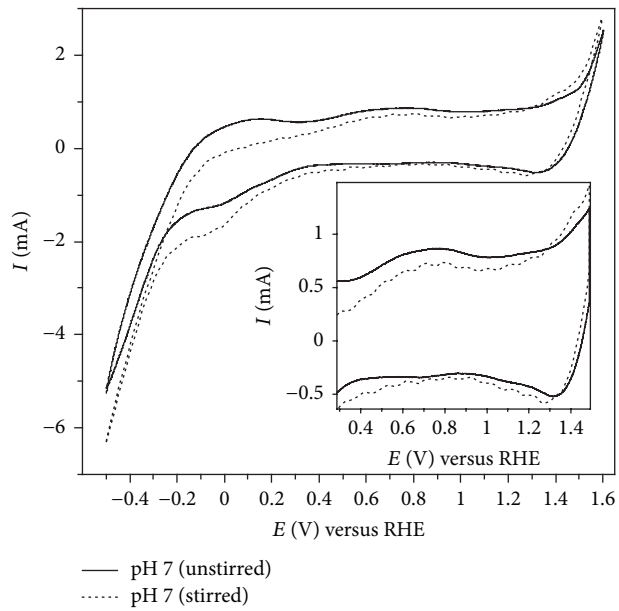

FIGURE 7: Hydrogen adsorption at a Ti/RuO_2 electrode in a stirred (300 min^{-1}) and unstirred pH 7 buffer solution. CE: platinum sheet.

quasi-hydrogen electrode, once a negative potential has been applied. The formally adsorbed hydrogen (even in the form of hydroxide species) is anodically oxidized according to the reversed equation (1). Cyclic voltammograms in the same solution with different starting potentials are shown in Figure 6.

A more cathodic electrode potential (in the hydrogen evolution direction) leads to (i) larger hydrogen oxidation currents and (ii) a shift of hydrogen oxidation towards more positive potentials. The impact of hydrogen on the behavior of a ruthenium oxide electrode was already mentioned in 1974 by Galizzioli et al. [11]. Continuous hydrogen evolution leads to the collapse of the atomic layers under the surface, but there is no lasting effect.

Michell et al. reported that hydrogen can adsorb in the lattice of the ruthenium oxide. This protonation of the oxide lattice leads to the formation of a large porous anodic film, which might break Ru-O bonds [16–18]. Today, we imagine proton insertion in RuO_2 by the dissociative adsorption of water [9] and bridged OH groups [10].

(1) In *acid solution*, the electrode potential increases with rising pH, in the same way that is known of the hydrogen oxidation at a hydrogen electrode. Protons are released by the dissociative adsorption of water and superacid OH groups. Simply, by the help of rutile lattice sites [Ru], the potential determining surface process at the more negatively charged RuO_2 electrode reads

$$\left[Ru^{III}\right]_2 O + H_2O \rightleftharpoons 2[Ru^{III}]OH \text{ or } [RuO]_2(H_2) \rightleftharpoons 2[Ru^{IV}]O + 2H^+ + 2e^- \quad (12)$$

Formally: $[Ru]\,H_2 \rightleftharpoons [Ru] + 2H^+ + 2e^-$

It is unclear whether Ru(II) exists during the anodic oxidation of hydrogen near 0 V according to (12). Figure 6 shows that the larger the potential is displaced in the negative direction, the higher the reversible oxidation and reduction currents of the Ru(III)/Ru(IV) couple at 0.5 V are.

(2) In *alkaline solution*, the electrode potential decreases with rising pH, in the same way that is known of the oxygen reduction at an oxygen electrode. By the dissociative adsorption of water, hydroxide sites are formed and bound in ruthenium cluster ions.

$$4\left[Ru^{IV}\right]O \text{ or } 2\,[Ru]_2(O_2) + 2H_2O + 4e^- \rightleftharpoons 2\left[Ru^{III}\right]_2 O + 4OH^- \quad (13)$$

Formally: $[Ru]\,O_2 + 4e^- + 2H_2O \rightleftharpoons [Ru] + 4OH^-$

If the potential is driven far in the positive direction, the oxygen reduction at 1.4 V and the Ru(IV) → Ru(III) reduction at 0.4 V get stronger. On the other hand, further oxidation states such as Ru(IV)/Ru(V) seem to be unaffected by the hydrogen insertion.

3.6. Diffusion Control. The fact that the hydrogen adsorption is a diffusion controlled reaction can be seen in Figure 7. The hydrogen region is clearly affected by stirring the solution, because the exchange of hydrogen ions between RuO_2 surface and solution is disturbed. This affects to a certain extent the oxidation of the electrode at 0.8 V, because H^+ is involved in the Ru(III)/Ru(IV) redox reaction.

4. Conclusion

This work compiles the impact of different acids and hydroxide solutions on the ruthenium dioxide electrode. With

respect to pH measurements, the determination of the OCP appears to be problematic in many respects, because the electrode potential varies in time and can hardly be reproduced due to hysteresis and aging effects.

Depending on the ionic strength, solutions even having the same pH and the same concentration cause different electrode potentials. Chloride ions affect strongly the behavior of the electrode. The cyclic voltammograms in acid solutions reveal alterations of the oxidation and reduction peaks due to interfering ions. In alkaline solution, the electrode seems to be affected by the potential window only.

We also demonstrated the hydrogen insertion into the bulk of the RuO_2, forming [Ru]-OH, which plays a role in the pH-dependent Ru(III)/Ru(IV) redox couple, whereas higher oxidation states remain unaffected.

This study shows that further work has to be done to understand in detail the impact of interfering ions on the pH response of a RuO_2 electrode.

Conflicts of Interest

The authors declare that they have no conflicts of interest.

References

[1] M. L. Hitchman and S. Ramanathan, "Potentiometric determination of proton activities in solutions containing hydrofluoric acid using thermally oxidized iridium electrodes," *Analyst*, vol. 116, no. 11, pp. 1131–1133, 1991.

[2] W. Vonau and U. Guth, "pH Monitoring: A review," *Journal of Solid State Electrochemistry*, vol. 10, no. 9, pp. 746–752, 2006.

[3] S. Gláb, A. Hulanicki, G. Edwall, F. Folke, I. Ingman, and W. F. Koch, "Metal-Metal Oxide and Metal Oxide Electrodes as pH Sensors," *Critical Reviews in Analytical Chemistry*, vol. 21, no. 1, pp. 29–47, 1989.

[4] P. Kurzweil, "Electrochemical Double-Layer Capacitors," in *Encyclopedia of Electrochemical Power Sources*, J. Garche, Ch. Dyer, P. Moseley, Z. Ogumi, D. Rand, and B. Scrosati, Eds., vol. 1, pp. 600–648, 665–678, Elsevier, Amsterdam, The Netherlands, 2009.

[5] M. Glanc-Gostkiewicz, M. Sophocleous, J. K. Atkinson, and E. Garcia-Breijo, "Performance of miniaturised thick-film solid state pH sensors," *Sensors and Actuators A: Physical*, vol. 202, pp. 2–7, 2013.

[6] L. Manjakkal, K. Zaraska, K. Cvejin, J. Kulawik, and D. Szwagierczak, "Potentiometric RuO2-Ta2O5 pH sensors fabricated using thick film and LTCC technologies," *Talanta*, vol. 147, pp. 233–240, 2016.

[7] W. Lonsdale, M. Wajrak, and K. Alameh, "RuO2 pH Sensor with Super-Glue-Inspired Reference Electrode," *Sensors*, vol. 17, no. 9, p. 2036, 2017.

[8] D. Janczak, A. Peplowski, G. Wroblewski, L. Gorski, E. Zwierkowska, and M. Jakubowska, "Investigations of Printed Flexible pH Sensing Materials Based on Graphene Platelets and Submicron RuO2 Powders," *Journal of Sensors*, vol. 2017, Article ID 2190429, 2017.

[9] P. Kurzweil, "Precious metal oxides for electrochemical energy converters: pseudocapacitance and pH dependence of redox processes," *Journal of Power Sources*, vol. 190, no. 1, pp. 189–200, 2009.

[10] H. Over, "Surface chemistry of ruthenium dioxide in heterogeneous catalysis and electrocatalysis: From fundamental to applied research," *Chemical Reviews*, vol. 112, no. 6, pp. 3356–3426, 2012.

[11] D. Galizzioli, F. Tantardini, and S. Trasatti, "Ruthenium dioxide: a new electrode material. I. Behaviour in acid solutions of inert electrolytes," *Journal of Applied Electrochemistry*, vol. 4, no. 1, pp. 57–67, 1974.

[12] J. Rumble, Ed., *CRC Handbook of Chemistry and Physics, , Taylor Fancis Ltd*, Taylor & Fancis Ltd, 98th edition, 2017.

[13] R. Kötz, S. Stucki, D. Scherson, and D. M. Kolb, "In-situ identification of RuO4 as the corrosion product during oxygen evolution on ruthenium in acid media," *Journal of Electroanalytical Chemistry*, vol. 172, no. 1-2, pp. 211–219, 1984.

[14] P. Kurzweil, J. Ober, and D. W. Wabner, "Method for extracting kinetic parameters from measured impedance spectra," *Electrochimica Acta*, vol. 34, no. 8, pp. 1179–1185, 1989.

[15] J. Soto, R. H. Labrador, M. D. Marcos et al., "A model for the assessment of interfering processes in Faradic electrodes," *Sensors and Actuators A: Physical*, vol. 142, no. 1, pp. 56–60, 2008.

[16] L. D. Burke, O. J. Murphy, J. F. O'Neill, and S. Venkatesan, "The oxygen electrode. Part 8. - Oxygen evolution at ruthenium dioxide anodes," *Journal of the Chemical Society, Faraday Transactions 1: Physical Chemistry in Condensed Phases*, vol. 73, pp. 1659–1671, 1977.

[17] L. D. Burke, J. K. Mulcahy, and S. Venkatesan, "An investigation of anodic film formation on electrodeposited ruthenium by potential sweep techniques," *Journal of Electroanalytical Chemistry*, vol. 81, no. 2, pp. 339–346, 1977.

[18] D. Michell, D. A. J. Rand, and R. Woods, "A study of ruthenium electrodes by cyclic voltammetry and x-ray emission spectroscopy," *Journal of Electroanalytical Chemistry*, vol. 89, pp. 11–27, 1978.